Composite Structures 94 (2012) 3781–3792

Contents lists available at SciVerse ScienceDirect

Composite Structures

journal homepage: www.elsevier.com/locate/compstruct

Studies on FRP-concrete interface with hardening and softening bond-slip law

Hong Yuan [a,*], Xusheng Lu [a], David Hui [b], Luciano Feo [c]

[a] MOE Key Lab of Disaster and Control in Engineering, Institute of Applied Mechanics, Jinan University, Guangzhou 510632, China
[b] Department of Mechanical Engineering, University of New Orleans, USA
[c] Department of Civil Engineering, University of Salerno, Italy

ARTICLE INFO

Article history:
Available online 18 June 2012

Keywords:
FRP
Harden
Soften
Load–displacement relationship
Ultimate load
Effective bond length

ABSTRACT

This latest experimental study proposes a theory that the bond-slip law for a FRP-concrete interface contains linear hardening and exponential softening. On the basis of this law, the paper studies the mechanic behavior and debonding process of a FRP-concrete interface. Firstly, through nonlinear fracture mechanics, the analytical solutions of the interface shear stress, the axial normal stress of FRP and the load–displacement relationship at the loaded end with the single shear test model of FRP-concrete are acquired. The shear stress propagation as well as the debonding process of the whole interface for different bond lengths could be predicted. Secondly, a simplified interface bond-slip law is used by changing the exponential softening law into a linear softening law. In addition, the analytical solutions for the simplified interface bond-slip law could also be obtained. Finally, based on the analytical solutions of the two bond-slip laws, the influences of the FRP bond length and stiffness on load–displacement curve and the ultimate load, as well as stiffness on effective bond length were discussed, with the similarities and differences between the two bond-slip laws also being studied.

1. Introduction

The functions of building structures could gradually become weaker due to both long term use and the natural environment. Studies show that fiber reinforced composite (Fiber Reinforced Polymer, referred to as FRP) reinforcements are an effective strengthening method, with them being given a great attention by the structural engineering industry.

At present, both domestic and foreign studies have been carried out on FRP reinforced concrete structures. The performance of the FRP-concrete interface is the base factor of this technique. The failure mode of FRP-reinforced beams is regularly related to the debonding of the FRP plate from the concrete. The debonding of the plate may take place either from the edge of the FRP strip or the intermediate flexural crack [1]. Based on single-lap shear specimens, Chajes et al. [2], Bizindavyi and Neale [3] studied the FRP-concrete interface bond strength and stress propagation. A constitutive law with the softening characteristics was proposed. Yoshizawa et al. [4] carried out several studies on the bond behavior of FRP-concrete based on single and double shear specimens. Nakaba [5] has carried out a lot of research on FRP-concrete debonding strength on double lap shear specimens. Yao et al. [6] studied the FRP-concrete interface shear strength based on single-shear tests. Among theoretical studies, Täljsten [7] used an elastic bond-slip model for FRP-concrete interface analysis. Brosens and Van Gemert [8] obtained the ultimate load for a linear softening bond-slip model. Yuan et al. [9] and Wu et al. [10] gave the ultimate load expression for different FRP and concrete widths. Using a simple three-parameter bond-slip constitutive model, Chirstopher KYL [11] divided the FRP-concrete interface into three regions, and obtained the shear stress distribution in each region. Teng et al. [12] used an elastic-softening bilinear bond-slip model to study the double shear FRP-concrete interface. Yuan et al. [13] used the same bond-slip model for the single side FRP reinforced concrete model to find the analytical solution of FRP-concrete interface. Analytical solutions in closed-form for the complete debonding process are also available for a local bond-slip law with linear softening [14] and nonlinear softening [15].

Based on the latest experimental results of a FRP-concrete interface with linear hardening and exponential softening bond-slip constitutive [16], this paper studies the FRP-concrete interface debonding process. Closed-form solutions are given.

2. Interface model of FRP-to-concrete

2.1. Interface model

The adhesive bonded joint analyzed, shown in Fig. 1, may be considered as a simple and typical model of FRP-strengthened structures in order to understand stress transfer and debonding behavior. The adhesive layer is mainly subjected to shear (mode

* Corresponding author. Tel./fax: +86 20 85228275.
E-mail address: tyuanhong@jnu.edu.cn (H. Yuan).

0263-8223/$ - see front matter © 2012 Elsevier Ltd. All rights reserved.
http://dx.doi.org/10.1016/j.compstruct.2012.06.009

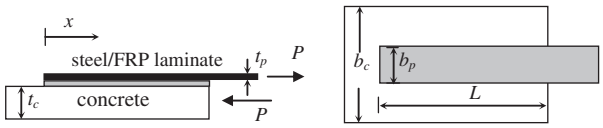

Fig. 1. Adhesive bonded joint.

II fracture). The thickness and width of the two layers are t_p and b_p for the upper steel/FRP laminate, and t_c and b_c for the lower concrete plate, respectively. The Young's moduli of the steell/FRP laminate and the concrete plate are E_p and E_c, repectively. L is the bonding length. Before starting the derivations, the following assumptions can made for the simplicity of problems:

- The adherents are homogeneous and linear elastic.
- The adhesive is only exposed to shear forces.
- Bending effects are neglected.
- The normal stresses are uniformly distributed over the cross-section.
- The thickness and width of the adherents are constant throughout the bond line.

2.2. Governing equations

Considering the element shown in Fig. 2, the equilibrium equations for adherents can be written as

$$\frac{d\sigma_p}{dx} - \frac{\tau}{t_p} = 0 \tag{1}$$

$$\sigma_p t_p b_p + \sigma_c t_c b_c = 0 \tag{2}$$

where τ is the shear stress in the adhesive layer. The constitutive equations for the adhesive layer and the two adherents are expressed as

$$\tau = f(\delta) \tag{3}$$

$$\sigma_p = E_p \frac{du_p}{dx} \tag{4}$$

$$\sigma_c = E_c \frac{du_c}{dx} \tag{5}$$

where u_p and u_c are the displacements of FRP and concrete.

The interface slip δ is defined as the relative displacement of two bonded layers.

$$\delta = u_p - u_c \tag{6}$$

Substituting (2)–(5) into (1) yields, by introducing two parameters of local bond strength τ_f and interfacial fracture energy G_f

$$\frac{d^2\delta}{dx^2} - \frac{2G_f}{\tau_f^2}\lambda^2 f(\delta) = 0 \tag{7}$$

$$\sigma_p = \frac{\tau_f^2}{2G_f t_p \lambda^2} \cdot \frac{d\delta}{dx} \tag{8}$$

where

$$\lambda^2 = \frac{\tau_f^2}{2G_f}\left(\frac{1}{E_p t_p} + \frac{b_p}{b_c E_c t_c}\right) \tag{9}$$

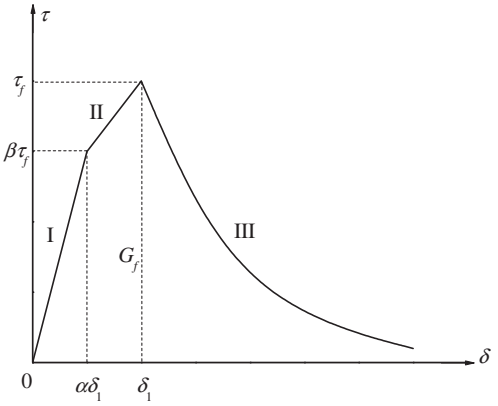

Fig. 3. Bond-slip law with exponential softening.

Equation (7) is the governing differential equation of the adhesive bonded joint in Fig. 1. When the local bond-slip law is found, this equation can be solved.

2.3. Bond-slip law

A study by a South Korean scientist shows how the local bond-slip law can be described as in Fig. 3. The interfacial shear stress increases linearly to $\beta\tau_f(\beta < 1)$ when the corresponding interface slip increases to $\alpha\delta_1(\alpha < 1)$. It is called an elastic state (state I). Then, the interfacial shear stress increases linearly to peak τ_f, while the interface slip increases from $\alpha\delta_1$ to δ_1. It is called a hardening state (state II). When the interface slip attains to δ_1, interface softening appears, and the interfacial shear stress decays exponentially with the interface slip. It is called a softening state (state III). The mathematical expressions of the interface bond-slip law in Fig. 3 are

$$f(\delta) = \begin{cases} \beta\frac{\tau_f}{\alpha\delta_1}\delta, & 0 \leqslant \delta \leqslant \alpha\delta_1 \\ \frac{\tau_f}{1-\alpha}\left[\frac{(1-\beta)\delta}{\delta_1} + (\beta-\alpha)\right], & \alpha\delta_1 < \delta \leqslant \delta_1 \\ \tau_f e^{\frac{-\tau_f}{k}(\delta-\delta_1)}, & \delta > \delta_1 \end{cases} \tag{10}$$

The bond-slip law in this paper is called the exponential model. G_f, the interfacial facture energy of the bond-slip law is the area enclosed by the curve and the δ axis in Fig. 3.

$$G_f = G_{f\mathrm{I}} + G_{f\mathrm{II}} + G_{f\mathrm{III}} = \frac{1}{2}(1-\alpha+\beta)\tau_f\delta_1 + k \tag{11}$$

where $G_{f\mathrm{I}}$, $G_{f\mathrm{II}}$ and $G_{f\mathrm{III}}$ are the areas under the curves, associated with the elastic, hardening and softening region, respectively. Based on the above bond-slip law, the interfacial shear stress, axial normal stress in FRP and the load–displacement relationship at the loaded end could be obtained.

In Fig. 4, the exponential softening model is simplified. When the interface slip increases to δ_1, softening appears, then the interface shear stress decreases linearly with the slip. When the interface slip attains to δ_f, the interfacial shear stress reduces to zero. It is called a debonding state (state IV). The mathematical expressions of the interface bond-slip law in Fig. 4 are

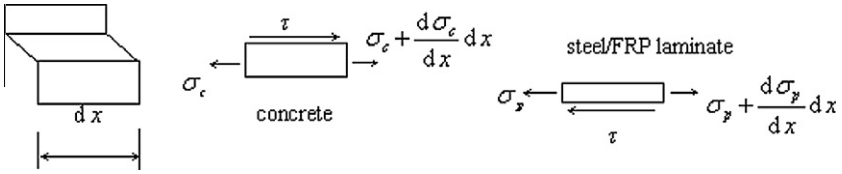

Fig. 2. Deformation and stresses of bonded joint.

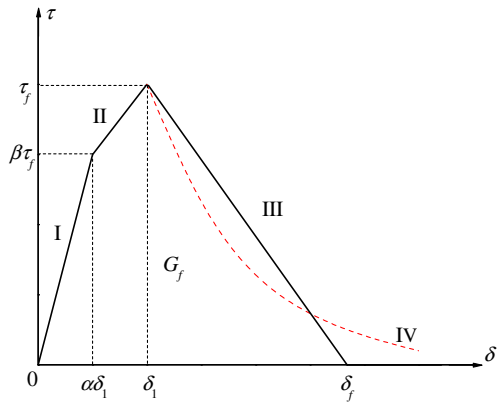

Fig. 4. Tri-linear bond-slip law.

$$f(\delta)=\begin{cases}\beta\frac{\tau_f}{\alpha\delta_1}\delta, & 0\leqslant\delta\leqslant\alpha\delta_1\\ \frac{\tau_f}{1-\alpha}\left[\frac{(1-\beta)\delta}{\delta_1}+(\beta-\alpha)\right], & \alpha\delta_1<\delta\leqslant\delta_1\\ -\frac{\tau_f}{\delta_f-\delta_1}(\delta-\delta_f), & \delta_1<\delta\leqslant\delta_f\\ 0, & \delta>\delta_f\end{cases} \tag{12}$$

The above bond-slip law is called a tri-linear model in the paper. The expression δ_f could be obtained by letting the interfacial fracture energy G_f in Figs. 3 and 4 be equal.

$$\delta_f=\frac{2k}{\tau_f}+\delta_1 \tag{13}$$

Based on the tri-linear model, the interfacial shear stress, axial normal stress in FRP and the load–displacement relationship at loaded end could also be obtained.

3. Analysis of the debonding process for the exponential model

3.1. Long bond length $L > h_0$

With the bond–slip model defined in Fig. 3, the governing equation (Eq. (7)) can be solved to find the shear stress distribution along the interface and the load–displacement response of the bonded joint. The solution can be presented below stage by stage with illustrations of the corresponding interfacial shear stress distribution and load–displacement curves. If the bond length L is longer than h_0, the failure process would experience an elastic stage, elastic-hardening stage, elastic-hardening–softening stage, hardening–softening stage and softening stage.

3.1.1. Elastic stage

When the load is low, with the interface shear stress at the end $x = L$ being less than $\beta\tau_f$, there is no hardening and softening. Substituting the relationship for $0\leqslant\delta\leqslant\alpha\delta_1$ in (10) into (7), the following is obtained:

$$\frac{d^2\delta}{dx^2}-\lambda_1^2\delta=0,\quad(0\leqslant\delta\leqslant\alpha\delta_1) \tag{14}$$

where

$$\lambda_1^2=\frac{2G_f}{\tau_f^2}\lambda^2\cdot\beta\frac{\tau_f}{\alpha\delta_1}=\frac{\beta\tau_f}{\alpha\delta_1}\left(\frac{1}{E_pt_p}+\frac{b_p}{b_cE_ct_c}\right) \tag{15}$$

with the boundary conditions

$$\sigma_p=0 \text{ at } x=0, \text{ and} \tag{16}$$
$$\sigma_p=P/(b_pt_p) \text{ at } x=L \tag{17}$$

The solution of Eq. (14) for the relative shear displacement, the shear stress of the adhesive layer as well as the normal stress of the laminate can be written in the form:

$$\delta=\frac{\alpha\delta_1}{\beta\tau_f}\cdot\frac{P\lambda_1\cosh(\lambda_1x)}{b_p\sinh(\lambda_1L)} \tag{18}$$
$$\tau=\frac{P\lambda_1}{b_p}\cdot\frac{\cosh(\lambda_1x)}{\sinh(\lambda_1L)} \tag{19}$$
$$\sigma_p=\frac{P}{b_pt_p}\cdot\frac{\sinh(\lambda_1x)}{\sinh(\lambda_1L)} \tag{20}$$

The interface slip Δ at the load end is defined as the displacement of the bonded joint. According to this definition, the relationship of the load–displacement from (18) can be obtained.

$$P=\frac{\beta\tau_fb_p}{\lambda_1}\cdot\frac{\Delta}{\alpha\delta_1}\tanh(\lambda_1L) \tag{21}$$

3.1.2. Elastic-hardening stage

As the load increases, the interface shear stress is greater than $\beta\tau_f$, but less than τ_f at $x = L$. The load P increases as the hardening length h increases. Substituting the relationship for $0\leqslant\delta\leqslant\alpha\delta_1$ and $\alpha\delta_1<\delta\leqslant\delta_1$ in (10) into (7), the following is obtained:

$$\frac{d^2\delta}{dx^2}-\lambda_1^2\delta=0,\quad(0\leqslant\delta\leqslant\alpha\delta_1) \tag{22}$$
$$\frac{d^2\delta}{dx^2}-\lambda_2^2\delta=\frac{\beta-\alpha}{1-\beta}\delta_1\lambda_2^2,\quad(\alpha\delta_1<\delta\leqslant\delta_1) \tag{23}$$

where λ_1^2 is given in Eq. (15), and

$$\lambda_2^2=\frac{2G_f}{\tau_f^2}\lambda^2\cdot\frac{1-\beta}{1-\alpha}\cdot\frac{\tau_f}{\delta_1}=\frac{1-\beta}{1-\alpha}\cdot\frac{\tau_f}{\delta_1}\left(\frac{1}{E_pt_p}+\frac{b_p}{b_cE_ct_c}\right) \tag{24}$$

with the boundary and continuous conditions

$$\sigma_p=0 \text{ at } x=0, \tag{25}$$
$$\sigma_p \text{ is continuous at } x=L-h, \tag{26}$$
$$\delta=\alpha\delta_1 \text{ at } x=L-h, \text{ and} \tag{27}$$
$$\sigma_p=P/(b_pt_p) \text{ at } x=L \tag{28}$$

Based on the boundary conditions (25) and (27), the solution of Eq. (22) for the relative shear displacement, the shear stress of the adhesive layer as well as the normal stress of the laminate can be written in the form:

$$\delta=\alpha\delta_1\frac{\cosh(\lambda_1x)}{\cosh[\lambda_1(L-h)]} \tag{29}$$
$$\tau=\beta\tau_f\frac{\cosh(\lambda_1x)}{\cosh[\lambda_1(L-h)]} \tag{30}$$
$$\sigma_p=\frac{\beta\tau_f}{t_p\lambda_1}\cdot\frac{\sinh(\lambda_1x)}{\cosh[\lambda_1(L-h)]} \tag{31}$$

Thus, based on the continuous condition (26) and boundary condition (27), the solution of Eq. (23) for the relative shear displacement, the shear stress of the adhesive layer as well as the normal stress of the laminate can be written in the form:

$$\delta=\frac{(1-\alpha)\beta\delta_1}{1-\beta}\cosh[\lambda_2(L-h-x)]-\frac{\alpha\delta_1\lambda_1}{\lambda_2}\tanh[\lambda_1(L-h)]\sinh[\lambda_2(L-h-x)]-\frac{\beta-\alpha}{1-\beta}\delta_1 \tag{32}$$

$$\tau=\beta\tau_f\cosh[\lambda_2(L-h-x)]-\frac{\alpha(1-\beta)\lambda_1\tau_f}{(1-\alpha)\lambda_2}\tanh[\lambda_1(L-h)]\sinh[\lambda_2(L-h-x)] \tag{33}$$

$$\sigma_p=-\frac{\beta\tau_f}{t_p\lambda_2}\sinh[\lambda_2(L-h-x)]+\frac{\beta\tau_f}{t_p\lambda_1}\tanh[\lambda_1(L-h)]\cosh[\lambda_2(L-h-x)] \tag{34}$$

Substituting the boundary condition (28) into (34), the following is obtained:

$$P=\frac{\beta b_p\tau_f}{\lambda_2}\sinh(\lambda_2h)+\frac{\beta b_p\tau_f}{\lambda_1}\tanh[\lambda_1(L-h)]\cosh(\lambda_2h) \tag{35}$$

The expression of the slip at the loaded end could be obtained from (32) when $x = L$

$$\Delta = \frac{(1-\alpha)\beta\delta_1}{1-\beta}\cosh(\lambda_2 h) + \frac{\alpha\delta_1\lambda_1}{\lambda_2}\tanh[\lambda_1(L-h)]\sinh(\lambda_2 h) - \frac{\beta-\alpha}{1-\beta}\delta_1 \quad (36)$$

At this stage, the load–displacement curve could be drawn from (35) and (36).

When the interface slip increases to δ_1 at $x = L$, interface softening appears at the loaded end. When considering a shorter bond length, the whole FRP-concrete interface is in hardening. Assuming h_0 covers the entire interface, then using the condition $\Delta = \delta_1$, the following is obtained:

$$\cosh(\lambda_2 h_0) = 1/\beta \quad (37)$$

3.1.3. Elastic-hardening–softening stage

As the load increases, the interface slip reaches δ_1, and the interface shear stress reaches the peak stress τ_f at $x = L$. The load P increased as the length of softening region a increased. Assuming the length of the hardening region is still expressed by h. Substituting the relationship in (10) into (7), the following is obtained:

$$\frac{d^2\delta}{dx^2} - \lambda_1^2\delta = 0, \quad (0 \leqslant \delta \leqslant \alpha\delta_1) \quad (38)$$

$$\frac{d^2\delta}{dx^2} - \lambda_2^2\delta = \frac{\beta-\alpha}{1-\beta}\delta_1\lambda_2^2, \quad (\alpha\delta_1 < \delta \leqslant \delta_1) \quad (39)$$

$$\frac{d^2\delta}{dx^2} - \lambda_3^2\frac{2k}{\tau_f}e^{\frac{-\tau_f}{k}\delta} = 0, \quad (\delta > \delta_1) \quad (40)$$

where λ_1^2 is given in (15), λ_2^2 is given in (24), and

$$\lambda_3^2 = \frac{2G_f}{\tau_f^2}\lambda^2 \cdot \tau_f e^{\frac{\tau_f}{k}\delta_1} \cdot \frac{\tau_f}{2k} = \frac{\tau_f^2}{2k}e^{\frac{\tau_f}{k}\delta_1}\left(\frac{1}{E_p t_p} + \frac{b_p}{b_c E_c t_c}\right) \quad (41)$$

with the boundary and continuous conditions

$$\sigma_p = 0 \text{ at } x = 0, \quad (42)$$

$$\delta = \alpha\delta_1 \text{ at } x = L - a - h, \quad (43)$$

$$\delta = \delta_1 \text{ at } x = L - a, \quad (44)$$

$$\sigma_p \text{ is continuous at } x = L - a - h, \quad (45)$$

$$\sigma_p \text{ is continuous at } x = L - a \quad (46)$$

$$\sigma_p = P/(b_p t_p) \text{ at } x = L \quad (47)$$

Based on the boundary conditions (42) and (43), the solution of Eq. (38) for the relative shear displacement, the shear stress of the adhesive layer and the normal stress of the laminate can be written in the form

$$\delta = \alpha\delta_1\frac{\cosh(\lambda_1 x)}{\cosh[\lambda_1(L-a-h)]} \quad (48)$$

$$\tau = \beta\tau_f\frac{\cosh(\lambda_1 x)}{\cosh[\lambda_1(L-a-h)]} \quad (49)$$

$$\sigma_p = \frac{\beta\tau_f}{t_p\lambda_1}\cdot\frac{\sinh(\lambda_1 x)}{\cosh[\lambda_1(L-a-h)]} \quad (50)$$

In addition, based on the boundary conditions (43) and (44), the solution of Eq. (39) for the relative shear displacement, the shear stress of the adhesive layer and the normal stress of the laminate can be written in the form

$$\delta = -\frac{(1-\alpha)\delta_1}{1-\beta}\cdot\frac{\sinh[\lambda_2(L-a-h-x)]}{\sinh(\lambda_2 h)} + \frac{(1-\alpha)\beta\delta_1}{1-\beta} \cdot\frac{\sinh[\lambda_2(L-a-x)]}{\sinh(\lambda_2 h)} - \frac{\beta-\alpha}{1-\beta}\delta_1 \quad (51)$$

$$\tau = -\tau_f\frac{\sinh[\lambda_2(L-a-h-x)]}{\sinh(\lambda_2 h)} + \beta\tau_f\frac{\sinh[\lambda_2(L-a-x)]}{\sinh(\lambda_2 h)} \quad (52)$$

$$\sigma_p = \frac{\tau_f}{t_p\lambda_2}\cdot\frac{\cosh[\lambda_2(L-a-h-x)]}{\sinh(\lambda_2 h)} - \frac{\beta\tau_f}{t_p\lambda_2}\cdot\frac{\cosh[\lambda_2(L-a-x)]}{\sinh(\lambda_2 h)} \quad (53)$$

Through the approach of reducing-order, the solution of Eq. (40) for the relative shear displacement, the shear stress of the adhesive layer and the normal stress of the laminate can be written in the form

$$\delta = \frac{2k}{\tau_f}\ln\{\cosh[\lambda_3\sqrt{c_1}(x-c_2)]\} - \frac{k}{\tau_f}\ln c_1 \quad (54)$$

$$\tau = \frac{c_1\tau_f e^{\frac{\tau_f}{k}\delta_1}}{\cosh^2[\lambda_3\sqrt{c_1}(x-c_2)]} \quad (55)$$

$$\sigma_p = \frac{\sqrt{c_1}\tau_f e^{\frac{\tau_f}{k}\delta_1}}{t_p\lambda_3}\tanh[\lambda_3\sqrt{c_1}(x-c_2)] \quad (56)$$

where the constants c_1 and c_2 could be determined by the boundary condition (44) and continuous condition (46).

$$c_1 = \frac{1}{4\lambda_3^2}\left[\frac{(1-\alpha)\tau_f\lambda_2\delta_1}{(1-\beta)k}\cdot\frac{\cosh(\lambda_2 h)-\beta}{\sinh(\lambda_2 h)}\right]^2 + e^{-\frac{\tau_f}{k}\delta_1} \quad (57)$$

$$c_2 = L - a - \frac{1}{2\lambda_3\sqrt{c_1}}\ln\frac{1+\sqrt{c_1 - e^{-\frac{\tau_f}{k}\delta_1}}/\sqrt{c_1}}{1-\sqrt{c_1 - e^{-\frac{\tau_f}{k}\delta_1}}/\sqrt{c_1}} \quad (58)$$

Substituting boundary condition (47) into (56), the following is obtained:

$$P = \frac{\sqrt{c_1}\tau_f b_p e^{\frac{\tau_f}{k}\delta_1}}{\lambda_3}\tanh[\lambda_3\sqrt{c_1}(L-c_2)] \quad (59)$$

The expression of the slip at the loaded end could be obtained from (54) when $x = L$,

$$\Delta = \frac{2k}{\tau_f}\ln\{\cosh[\lambda_3\sqrt{c_1}(L-c_2)]\} - \frac{k}{\tau_f}\ln c_1 \quad (60)$$

From the continuous condition (45), the relational expression between the hardening length h and the softening length a can be obtained.

$$\frac{\beta}{\lambda_1}\tanh[\lambda_1(L-a-h)] = \frac{1-\beta\cosh(\lambda_2 h)}{\lambda_2\sinh(\lambda_2 h)} \quad (61)$$

Thus, the load–displacement curve could be drawn from (59)–(61).

This stage either ends or the hardening–softening stage starts at $a + h = L$, then from (61), the following is obtained

$$\cosh(\lambda_2 h_{cr}) = 1/\beta \quad (62)$$

contrasted with (37), it is possible to know $h_{cr} = h_0$.

It is simple to know that only when the bond length L is greater than h_0, the interface debonding stages given above would appear one by one.

3.1.4. Hardening–softening stage

When the interface slip reaches $\alpha\delta_1$ at $x = 0$, the whole interface has both hardening and softening regions. The control differential equations in this stage are

$$\frac{d^2\delta}{dx^2} - \lambda_2^2\delta = \frac{\beta-\alpha}{1-\beta}\delta_1\lambda_2^2, \quad (\alpha\delta_1 \leqslant \delta \leqslant \delta_1) \quad (63)$$

$$\frac{d^2\delta}{dx^2} - \lambda_3^2\frac{2k}{\tau_f}e^{\frac{-\tau_f}{k}\delta} = 0, \quad (\delta > \delta_1) \quad (64)$$

where λ_2^2 is given in (24), λ_3^2 is given in (41), and with the boundary and continuous conditions

$$\sigma_p = 0 \text{ at } x = 0, \quad (65)$$

$$\delta = \delta_1 \text{ at } x = h = L - a, \quad (66)$$

$$\sigma_p \text{ is continuous at } x = h = L - a, \text{ and} \quad (67)$$

$$\sigma_p = P/(b_p t_p) \text{ at } x = L \quad (68)$$

Based on the boundary conditions (65) and (66), the solution of Eq. (63) for the relative shear displacement, the shear stress of the adhesive layer and the normal stress of the laminate can be written in the form

$$\delta = \frac{(1-\alpha)\delta_1}{1-\beta}\cdot\frac{\cosh(\lambda_2 x)}{\cosh(\lambda_2 h)} - \frac{(\beta-\alpha)\delta_1}{1-\beta} \tag{69}$$

$$\tau = \frac{\tau_f \cosh(\lambda_2 x)}{\cosh(\lambda_2 h)} \tag{70}$$

$$\sigma_p = \frac{\tau_f}{t_p\lambda_2}\cdot\frac{\sinh(\lambda_2 x)}{\cosh(\lambda_2 h)} \tag{71}$$

Similarly, from the boundary condition (66) and continuous condition (67), the solution of Eq. (64) for the relative shear displacement, the shear stress of the adhesive layer and the normal stress of the laminate can be written in the form

$$\delta = \frac{2k}{\tau_f}\ln\{\cosh[\lambda_3\sqrt{c_3}(x-c_4)]\} - \frac{k}{\tau_f}\ln c_3 \tag{72}$$

$$\tau = \frac{c_3\tau_f e^{\frac{\tau_f}{k}\delta_1}}{\cosh^2[\lambda_3\sqrt{c_3}(x-c_4)]} \tag{73}$$

$$\sigma_p = \frac{\sqrt{c_3}\tau_f e^{\frac{\tau_f}{k}\delta_1}}{t_p\lambda_3}\tanh[\lambda_3\sqrt{c_3}(x-c_4)] \tag{74}$$

where

$$c_3 = \frac{1}{4\lambda_3^2}\left[\frac{(1-\alpha)\tau_f\lambda_2\delta_1}{(1-\beta)k}\cdot\tanh(\lambda_2 h)\right]^2 + e^{-\frac{\tau_f}{k}\delta_1} \tag{75}$$

$$c_4 = h - \frac{1}{2\lambda_3\sqrt{c_3}}\ln\frac{1+\sqrt{c_3 - e^{-\frac{\tau_f}{k}\delta_1}}/\sqrt{c_3}}{1-\sqrt{c_3 - e^{-\frac{\tau_f}{k}\delta_1}}/\sqrt{c_3}} \tag{76}$$

Substituting the boundary condition (68) into (74), the following is obtained:

$$P = \frac{\sqrt{c_3}\tau_f b_p e^{\frac{\tau_f}{k}\delta_1}}{\lambda_3}\tanh[\lambda_3\sqrt{c_3}(L-c_4)] \tag{77}$$

The expression of the slip at the loaded end could be obtained from (72) when $x = L$,

$$\Delta = \frac{2k}{\tau_f}\ln\{\cosh[\lambda_3\sqrt{c_3}(L-c_4)]\} - \frac{k}{\tau_f}\ln c_3 \tag{78}$$

Thus, the load–displacement curve could be drawn from (77) and (78). This stage either ends or the softening stage starts at $h = 0$, then from (75)–(77) the load at this time is obtained.

$$P = \frac{\sqrt{e^{-\frac{\tau_f}{k}\delta_1}}\tau_f b_p e^{\frac{\tau_f}{k}\delta_1}}{\lambda_3}\tanh\left(\lambda_3 L\sqrt{e^{-\frac{\tau_f}{k}\delta_1}}\right) \tag{79}$$

3.1.5. Softening stage

When the interface slip reaches δ_1 at $x = 0$, the whole interface has only a softening region. The governing differential equation in this stage is

$$\frac{d^2\delta}{dx^2} - \lambda_3^2\frac{2k}{\tau_f}e^{-\frac{\tau_f}{k}\delta} = 0, \quad (\delta \geqslant \delta_1) \tag{80}$$

where λ_3^2 is given in (41).

The general solution of Eq. (80) is

$$\delta(x) = \frac{1}{2n}\ln\left\{\frac{1}{n}[e^{2x\sqrt{ne^{2nc_5}}+2c_6\sqrt{ne^{2nc_5}}+2nc_5} + 2m\sqrt{ne^{2nc_5}}e^{\sqrt{ne^{2nc_5}}(x+c_6)} + m^2 n]^2\right\} - 3c_5 - \frac{x}{n}\sqrt{ne^{2nc_5}} - \frac{c_6}{n}\sqrt{ne^{2nc_6}} - \frac{\ln 2}{n} \tag{81}$$

where c_5 and c_6 are constants,

$$m = 2k\lambda_3^2/\tau_f \tag{82}$$

$$n = \tau_f/k \tag{83}$$

The boundary conditions are

$$\sigma_p = 0 \text{ at } x = 0, \text{ and} \tag{84}$$

$$\sigma_p = P/(b_p t_p) \text{ at } x = a = L \tag{85}$$

Based on the boundary conditions, the following is obtained

$$\frac{(e^{2nc_5+2(L+c_6)\sqrt{ne^{2nc_5}}} - m^2 n)\sqrt{ne^{2nc_5}}}{n(e^{2nc_5+2(L+c_6)\sqrt{ne^{2nc_5}}} + m^2 n + 2m\sqrt{ne^{2nc_5}}e^{(L+c_6)\sqrt{ne^{2nc_5}}})} = \frac{2G_f\lambda^2 P}{\tau_f^2 b_p} \tag{86}$$

$$c_6 = -\frac{nc_5}{\sqrt{ne^{2nc_5}}} + \ln\frac{m^2 n}{2\sqrt{ne^{2nc_5}}} \tag{87}$$

From (86) and (87), the constants c_5 and c_6 could be determined, thus making it possible to obtain the general solution (81). Finally, the shear stress of the adhesive layer and the normal stress of the laminate can also be obtained. The expression of the slip at the loaded end could be obtained from (81) when $x = L$

$$\Delta = \frac{1}{2n}\ln\left\{\frac{1}{n}[e^{2L\sqrt{ne^{2nc_5}}+2c_6\sqrt{ne^{2nc_5}}+2nc_5} + 2m\sqrt{ne^{2nc_5}}e^{\sqrt{ne^{2nc_5}}(L+c_6)} + m^2 n]^2\right\} - 3c_5 - \frac{L}{n}\sqrt{ne^{2nc_5}} - \frac{c_6}{n}\sqrt{ne^{2nc_5}} - \frac{\ln 2}{n} \tag{88}$$

Thus, the load–displacement curve could be drawn from (86)–(88).

3.2. Short bond length $L < h_0$

The bond length L is longer than h_0 in the previous section. If the bond length L is shorter than h_0, as the slip equals $\alpha\delta_1$ at $x = 0$, the slip does not reach δ_1 at $x = L$, yet. The failure process would only experience an elastic stage, an elastic-hardening stage, a hardening stage, a hardening–softening stage, and a softening stage.

The elastic, elastic-hardening, hardening–softening and softening stages are the same as the corresponding stages in 3.1, thus the expressions of the interface slip, the interface shear stress, the normal stress of the laminate, and the relationship of the load–displacement are also the same. Only the hardening stage needs to be discussed further.

When the interface slip reaches $\alpha\delta_1$ at $x = 0$, the whole interface has only a hardening region. The governing differential equation in this stage is

$$\frac{d^2\delta}{dx^2} - \lambda_2^2\delta = \frac{\beta-\alpha}{1-\beta}\delta_1\lambda_2^2, \quad (\alpha\delta_1 \leqslant \delta \leqslant \delta_1) \tag{89}$$

where λ_2^2 is given in (24), and with the boundary conditions

$$\sigma_p = 0 \text{ at } x = 0, \text{ and} \tag{90}$$

$$\sigma_p = P/(b_p t_p) \text{ at } x = h = L \tag{91}$$

Based on the boundary conditions, the solution of Eq. (89) for the relative shear displacement, the shear stress of the adhesive layer and the normal stress of the laminate can be written in the form

$$\delta = \frac{P(1-\alpha)\delta_1\lambda_2\cosh(\lambda_2 x)}{(1-\beta)\tau_f b_p\sinh(\lambda_2 L)} - \frac{\beta-\alpha}{1-\beta}\delta_1 \tag{92}$$

$$\tau = \frac{P\lambda_2\cosh(\lambda_2 x)}{b_p\sinh(\lambda_2 L)} \tag{93}$$

$$\sigma_p = \frac{P\sinh(\lambda_2 x)}{t_p b_p\sinh(\lambda_2 L)} \tag{94}$$

The expression of the slip at the loaded end could be obtained from (92) when $x = L$,

$$\Delta = \frac{P(1-\alpha)\delta_1\lambda_2}{(1-\beta)\tau_f b_p\tanh(\lambda_2 L)} - \frac{\beta-\alpha}{1-\beta}\delta_1 \tag{95}$$

4. Analysis of the debonding process for the tri-linear model

Three values of critical bond length L_0, a_u, h_0 are identified with different failure process for the tri-linear model. These value are given as follows

$$L_0 = h_0 + a_0 \tag{96}$$

$$a = a_u = \frac{\pi}{2\lambda_4} \tag{97}$$

where h_0 is as shown in Eq. (37), λ_4 is given in (102), and

$$\tan(\lambda_4 a_0) = \frac{(\delta_f - \delta_1)\lambda_4\sqrt{1-\beta^2}}{(1-\alpha)(1+\beta)\lambda_2\delta_1} \tag{98}$$

4.1. Long bond length $L > L_0 = h_0 + a_0$

The failure process would experience an elastic stage, an elastic-hardening stage, an elastic-hardening–softening stage, an elastic-hardening–softening-debonding stage, a hardening–softening-debonding stage, and softening-debonding stage for long bond length $L > L_0$.

4.1.1. Elastic stage, elastic-hardening stage

The elastic and elastic-hardening stages are the same as the elastic stage as well as the elastic-hardening stage in 3.1, thus the expressions of the interface slip, the interface shear stress, the normal stress of the laminate, as well as the relationship of the load–displacement are also the same.

4.1.2. Elastic-hardening–softening stage

As the load increases, the interface slip reaches δ_1 at $x = L$, and interface softening appears at the loaded end, thus the whole interface is in the elastic-hardening–softening stage. The load P increased as the length of the softening region a increased. Assuming the length of the hardening region is still h. Substituting the relationship for $\delta < \delta_f$ in (12) into (7), the following is obtained:

$$\frac{d^2\delta}{dx^2} - \lambda_1^2\delta = 0, \quad (0 \leqslant \delta \leqslant \alpha\delta_1) \tag{99}$$

$$\frac{d^2\delta}{dx^2} - \lambda_2^2\delta = \frac{\beta-\alpha}{1-\beta}\delta_1\lambda_2^2, \quad (\alpha\delta_1 < \delta \leqslant \delta_1) \tag{100}$$

$$\frac{d^2\delta}{dx^2} + \lambda_4^2\delta = \delta_f\lambda_4^2, \quad (\delta_1 < \delta \leqslant \delta_f) \tag{101}$$

where λ_1^2 is given in (15), λ_2^2 is given in (24), and

$$\lambda_4^2 = \frac{2G_f}{\tau_f^2}\lambda^2 \cdot \frac{\tau_f}{\delta_f - \delta_1} = \frac{\tau_f}{\delta_f - \delta_1}\left(\frac{1}{E_p t_p} + \frac{b_p}{b_c E_c t_c}\right) \tag{102}$$

with the boundary and continuous conditions

$$\sigma_p = 0 \text{ at } x = 0, \tag{103}$$

$$\sigma_p \text{ is continuous at } x = L - a, \tag{104}$$

$$\delta = \delta_1 \text{ at } x = L - a, \tag{105}$$

$$\delta = \alpha\delta_1 \text{ at } x = L - a - h, \tag{106}$$

$$\sigma_p \text{ is continuous at } x = L - a - h, \text{ and} \tag{107}$$

$$\sigma_p = P/(b_p t_p) \text{ at } x = L \tag{108}$$

Based on the boundary conditions (103) and (106), the solution of Eq. (99) for the relative shear displacement, the shear stress of the adhesive layer and the normal stress of the laminate can be written in the form

$$\delta = \alpha\delta_1 \frac{\cosh(\lambda_1 x)}{\cosh[\lambda_1(L-a-h)]} \tag{109}$$

$$\tau = \beta\tau_f \frac{\cosh(\lambda_1 x)}{\cosh[\lambda_1(L-a-h)]} \tag{110}$$

$$\sigma_p = \frac{\beta\tau_f}{t_p\lambda_1} \cdot \frac{\sinh(\lambda_1 x)}{\cosh[\lambda_1(L-a-h)]} \tag{111}$$

In addition, based on the boundary conditions (105) and (106), the solution of Eq. (100) for the relative shear displacement, the shear stress of the adhesive layer and the normal stress of the laminate can be written in the form

$$\delta = -\frac{(1-\alpha)\delta_1}{1-\beta} \cdot \frac{\sinh[\lambda_2(L-a-h-x)]}{\sinh(\lambda_2 h)} + \frac{(1-\alpha)\beta\delta_1}{1-\beta} \cdot \frac{\sinh[\lambda_2(L-a-x)]}{\sinh(\lambda_2 h)} - \frac{\beta-\alpha}{1-\beta}\delta_1 \tag{112}$$

$$\tau = -\tau_f \frac{\sinh[\lambda_2(L-a-h-x)]}{\sinh(\lambda_2 h)} + \beta\tau_f \frac{\sinh[\lambda_2(L-a-x)]}{\sinh(\lambda_2 h)} \tag{113}$$

$$\sigma_p = \frac{\tau_f}{t_p\lambda_2} \cdot \frac{\cosh[\lambda_2(L-a-h-x)]}{\sinh(\lambda_2 h)} - \frac{\beta\tau_f}{t_p\lambda_2} \cdot \frac{\cosh[\lambda_2(L-a-x)]}{\sinh(\lambda_2 h)} \tag{114}$$

Finally, based on the continuous condition (104) and boundary condition (105), the solution of Eq. (101) for the relative shear displacement, the shear stress of the adhesive layer and the normal stress of the laminate can be written in the form

$$\delta = -\frac{(1-\alpha)\lambda_2\delta_1}{(1-\beta)\lambda_4} \cdot \frac{[\cosh(\lambda_2 h) - \beta]\sin[\lambda_4(L-a-x)]}{\sinh(\lambda_2 h)} - (\delta_f - \delta_1)\cos[\lambda_4(L-a-x)] + \delta_f \tag{115}$$

$$\tau = \frac{(1-\alpha)\lambda_2\delta_1\tau_f}{(1-\beta)\lambda_4(\delta_f - \delta_1)} \cdot \frac{[\cosh(\lambda_2 h) - \beta]\sin[\lambda_4(L-a-x)]}{\sinh(\lambda_2 h)} + \tau_f\cos[\lambda_4(L-a-x)] \tag{116}$$

$$\sigma_p = \frac{\tau_f}{\lambda_2 t_p} \cdot \frac{[\cosh(\lambda_2 h) - \beta]\cos[\lambda_4(L-a-x)]}{\sinh(\lambda_2 h)} - \frac{\tau_f}{\lambda_3 t_p}\sin[\lambda_4(L-a-x)] \tag{117}$$

Substituting the boundary condition (108) into (117), the following is obtained:

$$P = \frac{\tau_f b_p}{\lambda_2} \cdot \frac{[\cosh(\lambda_2 h) - \beta]\cos(\lambda_4 a)}{\sinh(\lambda_2 h)} + \frac{\tau_f b_p}{\lambda_3}\sin(\lambda_4 a) \tag{118}$$

The expression of the slip at the loaded end could be obtained from (115) when $x = L$,

$$\Delta = \frac{(1-\alpha)\lambda_2\delta_1}{(1-\beta)\lambda_4} \cdot \frac{[\cosh(\lambda_2 h) - \beta]\sin(\lambda_4 a)}{\sinh(\lambda_2 h)} - (\delta_f - \delta_1) \times \cos(\lambda_4 a) + \delta_f \tag{119}$$

From the continuous condition (107), the relational expression between the hardening length h and the softening length a is obtained.

$$\frac{\beta}{\lambda_1}\tanh[\lambda_1(L-a-h)] = \frac{1-\beta\cosh(\lambda_2 h)}{\lambda_2\sinh(\lambda_2 h)} \tag{120}$$

Thus, the load–displacement curve could be drawn from (118)–(120). When this stage either ends or the elastic-hardening–softening-debonding stage begins as $\Delta = \delta_f$ in (119), the following is obtained:

$$\frac{(1-\alpha)\lambda_2\delta_1}{(1-\beta)\lambda_4} \cdot \frac{[\cosh(\lambda_2 h) - \beta]\tan(\lambda_4 a)}{\sinh(\lambda_2 h)} - (\delta_f - \delta_1) = 0 \tag{121}$$

4.1.3. Elastic-hardening–softening-debonding stage

At this stage, debondings (or macro-cracks or breaks) appear and extend along the interface. When $\Delta > \delta_f$, the bond length keeps decreasing as the cracks extend. When crack extending occurs, the FRP-concrete interface is in the elastic-hardening–softening-debonding stage, and the shear stress peak τ_f moves towards the free end of the lap joint. Assuming that the debonding length of the loaded end was d, substituting L as L-d, equations (109)–(118), (120) and (121) were still correct.

When $\delta > \delta_f$, displacement of the loaded end could be obtained from solving (7), or simply gained by stacking all the displacements of the lap joint, the relationship between load and displacement is

$$\Delta = \delta_f + \left(\frac{P}{E_p t_p b_p} + \frac{P}{E_c t_c b_c}\right) d = \delta_f + \frac{Pd\lambda^2}{\tau_f b_p}[(1-\alpha+\beta)\delta_1 + \delta_f] \tag{122}$$

The elastic-hardening–softening-debonding stage can only appear when the free end is still in an elastic state before debonding begins at the loaded end. Considering a critical situation, hardening appears at the free end while debonding begins at the loaded end. Therefore, $L = a + h$ and $h = h_0$ is obtained from equation (120), which is the same as Eq. (37). Substitutiong this value of h into (121) yields a_0 as expressed in (98).

It is possible to claim that, only when the bond length $L > L_0 = h_0 + a_0$, the above interfacial shear stress distribution is completely correct and all the stages of the debonding process will appear stage by stage.

4.1.4. Hardening–softening-debonding stage

When the interface slip reaches $\alpha\delta_1$ at $x = 0$, the FRP-concrete interface is in the hardening–softening -debonding stage, the equation at this stage is:

$$\frac{d^2\delta}{dx^2} - \lambda_2^2\delta = \frac{\beta-\alpha}{1-\beta}\delta_1\lambda_2^2, \quad (\alpha\delta_1 \leqslant \delta \leqslant \delta_1) \tag{123}$$

$$\frac{d^2\delta}{dx^2} + \lambda_4^2\delta = \delta_f\lambda_4^2, \quad (\delta_1 < \delta \leqslant \delta_f) \tag{124}$$

where λ_2^2 is given in (24), and λ_4^2 is given in (102).

The boundary and continuous conditions are

$$\sigma_p = 0 \text{ at } x = 0 \tag{125}$$

$$\delta = \delta_1 \text{ at } x = h = L - a - d, \tag{126}$$

$$\delta = \delta_f, \text{ at } x = a + h = L - d, \tag{127}$$

$$\sigma_p \text{ is continuous at } x = h = L - a - d \tag{128}$$

$$\sigma_p = P/t_p b_p \text{ at } x = a + h = L - d \tag{129}$$

Based on the boundary conditions (125) and (126), the solution of Eq. (123) for the relative shear displacement, the shear stress of the adhesive layer and the normal stress of the laminate can be written in the form:

$$\delta = \frac{(1-\alpha)\delta_1}{1-\beta}\cdot\frac{\cosh(\lambda_2 x)}{\cosh(\lambda_2 h)} - \frac{(\beta-\alpha)\delta_1}{1-\beta} \tag{130}$$

$$\tau = \frac{\tau_f \cosh(\lambda_2 x)}{\cosh(\lambda_2 h)} \tag{131}$$

$$\sigma_p = \frac{\tau_f}{t_p\lambda_2}\cdot\frac{\sinh(\lambda_2 x)}{\cosh(\lambda_2 h)} \tag{132}$$

In addition, based on the boundary conditions (126) and (127), the solution of Eq. (124) for the relative shear displacement, the shear stress of the adhesive layer and the normal stress of laminate can be written in the form:

$$\delta = \delta_f - \frac{\delta_f - \delta_1}{\sin(\lambda_4 a)}\sin[\lambda_4(a + h - x)] \tag{133}$$

$$\tau = \frac{\tau_f}{\sin(\lambda_4 a)}\sin[\lambda_4(a + h - x)] \tag{134}$$

$$\sigma_p = \frac{\tau_f}{t_p\lambda_4}\cdot\frac{\cos[\lambda_4(a + h - x)]}{\sin(\lambda_4 a)} \tag{135}$$

From the boundary condition (129), the following is obtained:

$$P = \frac{\tau_f b_p}{\lambda_4 \sin(\lambda_4 a)} \tag{136}$$

And the load–displacement relationship could be obtained by superposition:

$$\Delta = \delta_f + \frac{Pd\lambda^2}{\tau_f b_p}[(1-\alpha+\beta)\delta_1 + \delta_f] \tag{137}$$

Substituting (132) and (135) into the continuous condition (128), the relationship of the hardening area length h and the softening area length a could be obtained as:

$$\frac{1}{\lambda_2}\tanh(\lambda_2 h) = \frac{1}{\lambda_4}\cot(\lambda_4 a) \tag{138}$$

At the end of this stage, or the beginning of the softening-debonding stage, as $h = 0$, that is

$$a = a_u = \frac{\pi}{2\lambda_4} \tag{139}$$

This is the minimum bond length for the softening-debonding stage to appear.

4.1.5. Softening-debonding stage

When $x = 0$, as the interface slip reaches δ_1, the FRP-concrete interface is in the softening-debonding stage, the equation at this stage is:

$$\frac{d^2\delta}{dx^2} + \lambda_4^2\delta = \delta_f\lambda_4^2, \quad (\delta_1 \leqslant \delta \leqslant \delta_f) \tag{140}$$

where λ_4^2 is given in (102).

The boundary conditions are:

$$\sigma_p = 0 \text{ at } x = 0 \tag{141}$$

$$\sigma_p = P/t_p b_p \text{ at } x = a = L - d, \tag{142}$$

$$\delta = \delta_f, \text{ at } x = a = L - d, \tag{143}$$

Based on the boundary conditions (141) and (142), the solution of Eq. (140) for the relative shear displacement, the shear stress of the adhesive layer and the normal stress of the laminate can be written in the form:

$$\delta = \delta_f - \frac{P\lambda_4(\delta_f - \delta_1)}{\tau_f b_p}\cdot\frac{\cos(\lambda_4 x)}{\sin(\lambda_4 a)} \tag{144}$$

$$\tau = \frac{P\lambda_4}{b_p}\cdot\frac{\cos(\lambda_4 x)}{\sin(\lambda_4 a)} \tag{145}$$

$$\sigma_p = \frac{P}{t_p b_p}\cdot\frac{\sin(\lambda_4 x)}{\sin(\lambda_4 a)} \tag{146}$$

Eq. (139) could also be obtained from the boundary condition (143), that is, the softening area length is constant a_u during the whole softening-debonding stage. The load–displacement relationship is

$$\Delta = \delta_f + \frac{P\lambda^2(L - a_u)}{\tau_f b_p}[(1-\alpha+\beta)\delta_1 + \delta_f] \tag{147}$$

4.2. Short bond length $L < h_0$

If the bond length L is shorter than h_0, as the slip at $x = 0$ attains to $\alpha\delta_1$, the slip at $x = L$ is still less than δ_1. The failure process would

only experience an elastic stage, an elastic-hardening stage, a hardening stage, a hardening–softening stage, a softening stage.

4.2.1. Elastic stage, elastic-hardening stage, hardening stage

The elastic and elastic-hardening stages are the same as the corresponding stages in 3.1, and the hardening stage is the same as the corresponding stage in 3.2, thus the expressions of the interface slip, the interface shear stress, the normal stress of the laminate, and the relationship of the load–displacement are also the same. Only the hardening–softening and softening stages need to be discussed further.

4.2.2. Hardening–softening stage

When the interface slip reaches δ_1 at $x = L$, the whole interface has both hardening and softening regions. The governing differential equations in this stage are:

$$\frac{d^2\delta}{dx^2} - \lambda_2^2\delta = \frac{\beta-\alpha}{1-\beta}\delta_1\lambda_2^2, \quad (\alpha\delta_1 \leqslant \delta \leqslant \delta_1) \tag{148}$$

$$\frac{d^2\delta}{dx^2} + \lambda_4^2\delta = \delta_f\lambda_4^2, \quad (\delta_1 < \delta \leqslant \delta_f) \tag{149}$$

where λ_2^2 is given in (24), λ_4^2 is given in (102), and with the boundary and continuous conditions

$$\sigma_p = 0 \text{ at } x = 0, \tag{150}$$

$$\sigma_p \text{ is continus at } x = h = L - a, \tag{151}$$

$$\delta = \delta_1 \text{ at } x = h = L - a, \text{ and} \tag{152}$$

$$\sigma_p = P/(b_p t_p) \text{ at } x = L \tag{153}$$

Based on the boundary conditions (150) and (152), the solution of Eq. (148) for the relative shear displacement, the shear stress of the adhesive layer and the normal stress of the laminate can be written in the form:

$$\delta = \frac{(1-\alpha)\delta_1\cosh(\lambda_2 x)}{(1-\beta)\cosh[\lambda_2(L-a)]} - \frac{\beta-\alpha}{1-\beta}\delta_1 \tag{154}$$

$$\tau = \frac{\tau_f\cosh(\lambda_2 x)}{\cosh[\lambda_2(L-a)]} \tag{155}$$

$$\sigma_p = \frac{\tau_f\sinh(\lambda_2 x)}{\lambda_2 t_p\cosh[\lambda_2(L-a)]} \tag{156}$$

Based on the continuous condition (151) and boundary condition (152), the solution of Eq. (149) for the relative shear displacement, the shear stress of the adhesive layer and the normal stress of laminate can be written in the form:

$$\delta = \delta_f - (\delta_f - \delta_1)\cos[\lambda_4(L-a-x)] - \frac{(1-\alpha)\lambda_2\delta_1}{(1-\beta)\lambda_4}\tanh[\lambda_2(L-a)]\sin[\lambda_4(L-a-x)] \tag{157}$$

$$\tau = \tau_f\cos[\lambda_4(L-a-x)] + \frac{(1-\alpha)\lambda_2\delta_1\tau_f}{(1-\beta)(\delta_f-\delta_1)\lambda_4}\tanh[\lambda_2(L-a)]\sin[\lambda_4(L-a-x)] \tag{158}$$

$$\sigma_p = -\frac{\tau_f}{t_p\lambda_4}\sin[\lambda_4(L-a-x)] + \frac{\tau_f}{t_p\lambda_2}\tanh[\lambda_2(L-a)]\cos[\lambda_4(L-a-x)] \tag{159}$$

Substituting the boundary condition (153) into (159) yields

$$P = \frac{b_p\tau_f}{\lambda_4}\sin(\lambda_4 a) + \frac{b_p\tau_f}{\lambda_2}\tanh[\lambda_2(L-a)]\cos(\lambda_4 a) \tag{160}$$

The expression of the slip at the loaded end could be obtained from (157) when $x = L$

$$\Delta = \delta_f - (\delta_f - \delta_1)\cos(\lambda_4 a) + \frac{(1-\alpha)\lambda_2\delta_1}{(1-\beta)\lambda_4}\tanh[\lambda_2(L-a)]\sin(\lambda_4 a) \tag{161}$$

Thus, the load–displacement curve could be drawn from (160) and (161). A critical bond length can be obtained when the interface slip reaches δ_f at $x = L$ and $L = a$, which gives $L = a_u$.

4.2.3. Softening stage

When the interface slip reaches δ_1 at $x = 0$, the whole interface only has a softening region. The governing differential equation in this stage is:

$$\frac{d^2\delta}{dx^2} + \lambda_4^2\delta = \delta_f\lambda_4^2, \quad (\delta_1 \leqslant \delta \leqslant \delta_f) \tag{162}$$

where λ_4^2 is given in (102), and with the boundary condition

$$\sigma_p = 0 \text{ at } x = 0, \text{ and} \tag{163}$$

$$\sigma_p = P/(b_p t_p) \text{ at } x = a = L \tag{164}$$

Based on the boundary conditions (163) and (164), the solution of Eq. (162) for the relative shear displacement, the shear stress of the adhesive layer and the normal stress of the laminate can be written in the form:

$$\delta = \delta_f - \frac{P(\delta_f-\delta_1)\lambda_4}{b_p\tau_f\sin(\lambda_4 L)}\cos(\lambda_4 x) \tag{165}$$

$$\tau = \frac{P\lambda_4}{b_p\sin(\lambda_4 L)}\cos(\lambda_4 x) \tag{166}$$

$$\sigma_p = \frac{P\sin(\lambda_4 x)}{t_p b_p\sin(\lambda_4 L)} \tag{167}$$

The load P at the beginning of this stage could be obtained from the boundary condition $\delta|_{x=0} = \delta_1$, as follows,

$$P = \frac{\tau_f b_p}{\lambda_4}\sin(\lambda_4 L) \tag{168}$$

The expression of the slip at the loaded end could be obtained from (165) when $x = L$

$$\Delta = \delta_f - \frac{P(\delta_f-\delta_1)\lambda_4}{b_p\tau_f\tan(\lambda_4 L)} \tag{169}$$

4.3. Bond length $h_0 < L < a_u$

If the bond length L is shorter than a_u and longer than h_0, the failure process would experience an elastic stage, an elastic-hardening stage, an elastic-hardening–softening stage, a hardening–softening stage, as well as a softening stage.

All the aforementioned stages are discussed in the previous sections and the closed-form solutions are obtained, thus the expressions of the interface slip, the interface shear stress, the normal stress of the laminate, and the relationship of the load–displacement are also the same.

4.4. Bond length $a_u < L < l_0$

If the bond length L is longer than a_u and shorter than l_0, the failure process would experience an elastic stage, an elastic-hardening stage, an elastic-hardening–softening stage, a hardening–softening stage, a hardening–softening-debonding stage, and a softening-debonding stage.

All the stages above are discussed in the previous sections and the closed-form solutions are obtained, thus the expressions of the interface slip, the interface shear stress, the normal stress of the

laminate, and the relationship of the load–displacement are the same.

5. Numerical simulations

The material properties and geometry parameters in the numerical analysis are selected as follows: $t_p = 1.4$ mm, $b_p = 30$ mm, $t_c = 200$ mm, $b_c = 200$ mm, $E_p = 152.2$ Gpa, $E_c = 32.5$ Gpa. And the interfacial characteristic parameters are selected as $\alpha = 0.5$, $\beta = 0.7$, $k = 0.8$ N/mm, $\delta_1 = 0.07$ mm, $\tau_f = 5.6$ Mpa.

It could be obtained that $\delta_f = 0.3557$ mm, $h_0 = 59.5$ m, $a_0 = 118.9$ mm, $a_u = 163.4$ mm, $l_0 = h_0 + a_0 = 178.4$ mm. According to the above analysis, the failure process for different bond lengths could be discussed.

5.1. Load–displacement curves

5.1.1. Load–displacement curves of the exponential model

When the bond length $L > h_0$, take $L = 100$ mm, the load–displacement curve is shown in Fig. 5(a). OA is the elastic stage, AB is the elastic-hardening stage, BC is the elastic-hardening–softening stage, CD is the hardening–softening stage, and DE is the softening stage.

When the bond length $L < h_0$, take $L = 50$ mm, the load–displacement curve of this situation is shown in Fig. 5b. OA is the elastic stage, AB is the elastic-hardening stage, BC is the hardening stage, CD is the hardening–softening stage, and DE is the softening stage.

5.1.2. Load–displacement curves of the tri-linear model

When bond length $L > l_0$, take $L = 200$ mm, the load–displacement curve is shown in Fig. 6a. OA is the elastic stage, AB is the elastic-hardening stage, BC is the elastic-hardening–softening stage, CD is the elastic-hardening–softening-debonding stage, DE is the hardening–softening-debonding stage, and EF is the softening-debonding stage.

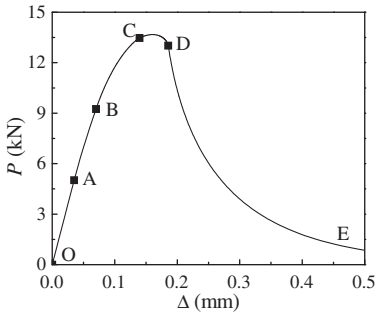

(a) L=100mm

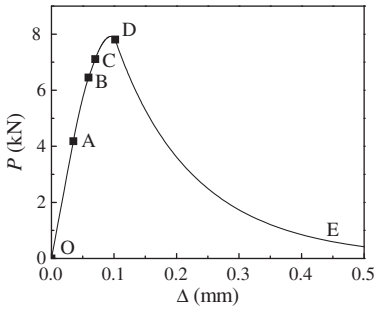

(b) L=50mm

Fig. 5. Load–displacement curves.

When the bond length $a_u < L < l_0$, take $L = 170$ mm, the load–displacement curve is shown in Fig. 6b. OA is the elastic stage, AB is the elastic-hardening stage, BC is the elastic-hardening–softening stage, CD is the hardening–softening stage, DE is the hardening–softening-debonding stage, and EF is the softening-debonding stage.

When the bond length $h_0 < L < a_u$, take $L = 100$ mm, the load–displacement curve is shown in Fig. 6c. OA is the elastic stage, AB

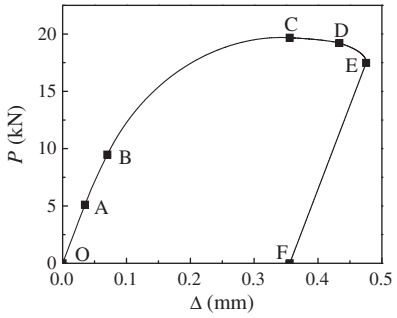

(a) L=200mm

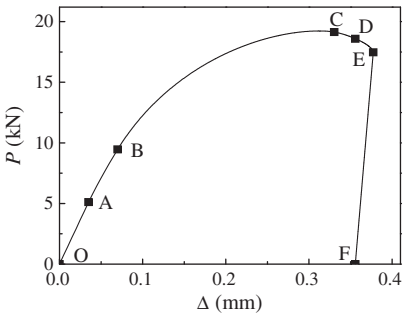

(b) L=170mm

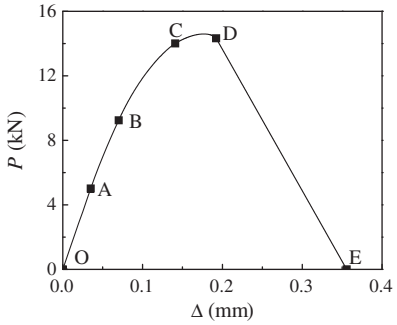

(c) L=100mm

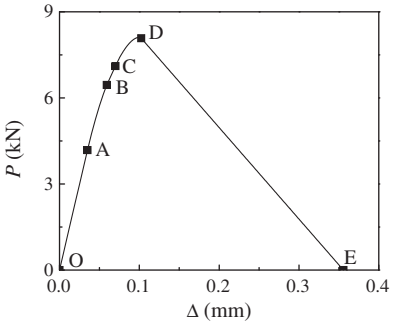

(d) L=50mm

Fig. 6. Load–displacement curves.

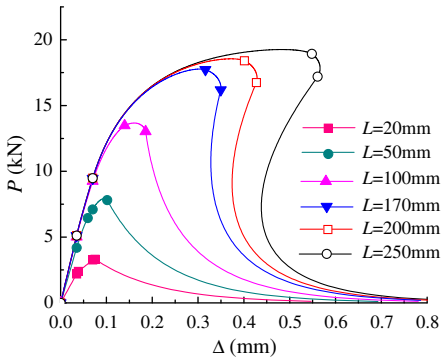

Fig. 7. Load–displacement curves of the exponential model for the different bond lengths.

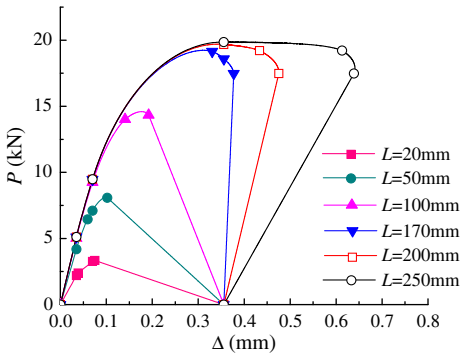

Fig. 8. The load–displacement curves of the tri-linear model for different bond lengths.

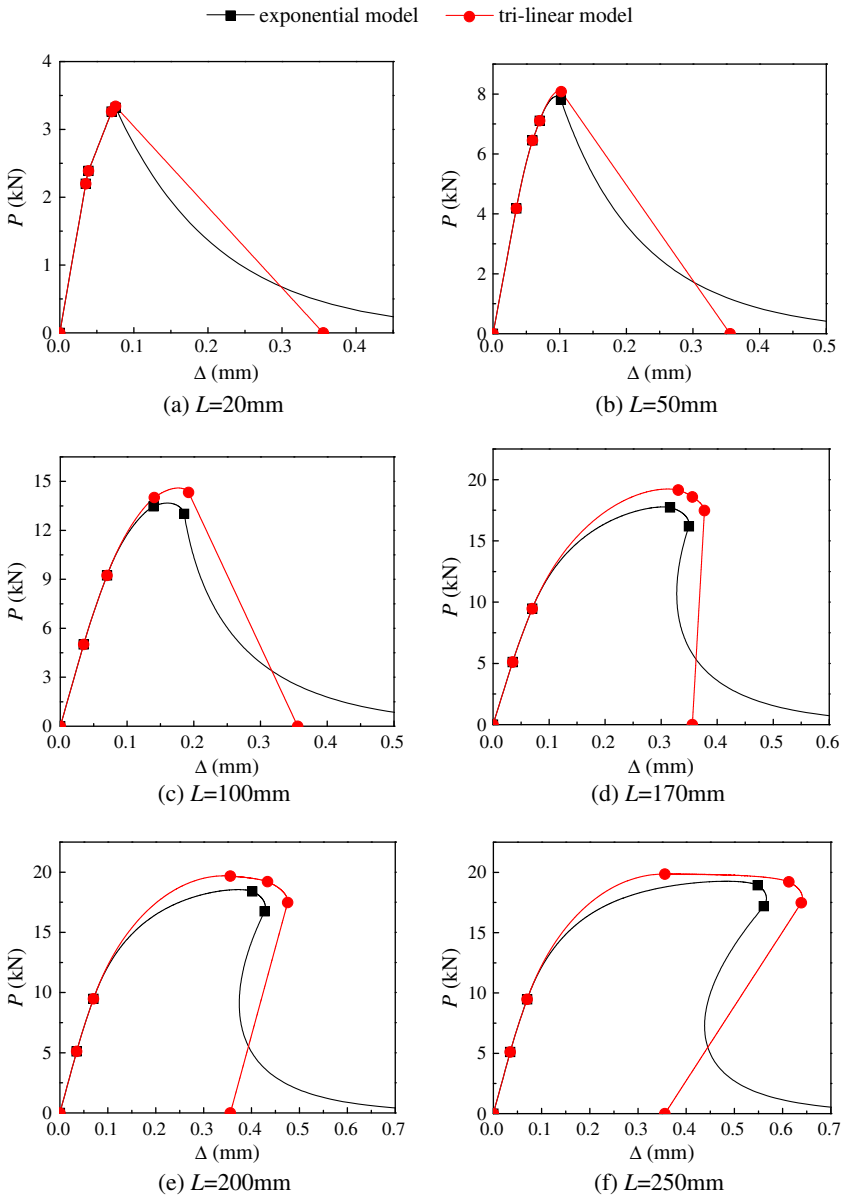

Fig. 9. Comparison of the load–displacement curves of the two models for different bond lengths.

is the elastic-hardening stage, BC is the elastic-hardening–softening stage, CD is the hardening–softening stage, and DE is the softening stage.

When the bond length $L < h_0$, take $L = 50$ mm, the load–displacement curve is shown in Fig. 6d. OA is the elastic stage, AB is the elastic-hardening stage, BC is the hardening stage, CD is the hardening–softening stage, and DE is the softening stage.

5.2. Parametric study

Fig. 7 shows the influence for different bond lengths of the exponential model on the load–displacement curves. From the figure, the significant influence for the bond lengths on the curves could be observed. As the bond length increased, not only would the interface failure processes change, but so would the ultimate load and interface slip. Specifically, the increase of the bond length can increase damage ductility. However, when the bond length reaches a certain length (effective bond length), the ultimate load would hardly change.

Fig. 8 shows the influence for different bond lengths of the tri-linear model on the load–displacement curves. From the figure, the significant influence for bond lengths on the curves could also be observed. In the range of the effective bond length, as the bond length increased, not only would the interface failure processes change, but so would the ultimate load and interface slip. Namely, the increase of the bond length can increase damage ductility.

Fig. 9 shows the comparison of the load–displacement curves between the exponential model and the tri-linear model for the different bond lengths. From the figure, the load would increase faster in the tri-linear model as the bond length increases. The load–displacement curves would be different when a softening area exists. In addition, since there is no debonding situation in the exponential model, the displacement would increase unlimitedly, with this being different from the tri-linear model in which the slip would approach δ_f.

Fig. 10 shows the load–displacement curves of the exponential model for different FRP stiffnesses. From the figure, the significant influence for FRP stiffness to the curves could be observed. As the stiffness increases, the ultimate load increases. However, the slip would decrease, namely the ductility reduced.

Fig. 11 shows the load–displacement curves of the tri-linear model for different FRP stiffnesses. From the figure, the significant influence for FRP stiffness on the curves could also be observed. As the stiffness increases, the ultimate load increases. However the slip would decrease, namely the ductility reduced.

Through the numerical computation, the ultimate load of exponential and tri-linear models for different bond lengths could be obtained. Fig. 12 shows the ultimate load for different bond lengths. From the figure, in the tri-linear model, when the bond length is smaller, the ultimate load increased significantly with the bond length. When the bond length is greater, the ultimate load stayed essentially unchanged. In the exponential model, when the bond length is smaller, the trend is similar to the tri-linear model, but its ultimate load is relatively smaller. Both models have the same ultimate load when the bond length is relatively large.

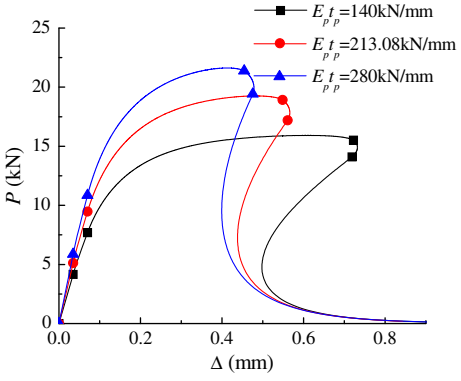

Fig. 10. Load–displacement curves of the exponential model for different FRP stiffnesses.

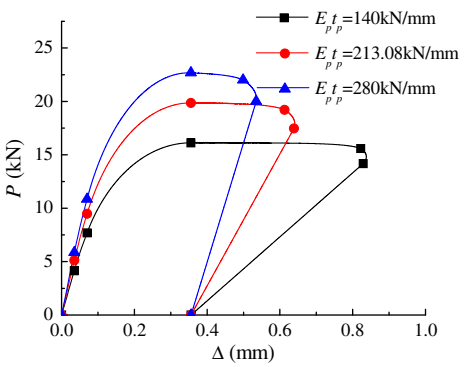

Fig. 11. The load–displacement curves of the tri-linear model for different FRP stiffness.

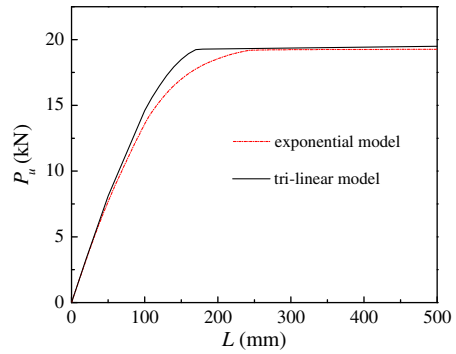

Fig. 12. The ultimate load for different bond lengths.

6. Conclusions

The FRP-concrete interface debonding process and mechanical behavior are the key issues of FRP-concrete reinforced technology. A study of the FRP-concrete interface debonding process and the mechanical behavior was carried out, with it being based on the latest experimental results on FRP-concrete interfaces with bond-slip laws which contain an exponential softening and a linear hardening constitutive relations. Through nonlinear fracture mechanics, the analytical expressions of the interfacial shear stress, the axial normal stress in FRP and the load–displacement relationship at the loaded end of the FRP-to-concrete interface with single shear test model could be obtained. Thus, the shear stress propagation and debonding process of the whole interface for different bond lengths could be predicted. Through the analytical solutions of the two bond-slip laws, the influences of different FRP bond lengths and stiffness on the load–displacement curve, and the ultimate load were studied. The stress transfer mechanism, the interface crack propagation and the ductility behavior of the joint could be explained. In addition, the similarities and differences between the two bond-slip laws were also studied. On the basis of fully understanding the FRP-concrete interfacial mechanical behavior, the full-range behavioral characteristics and the crucial factors of the FRP-concrete interfacial debonding problem can be understood

in greater detail, with it providing a reliable theoretical basis for concrete FRP strengthening technology.

Acknowledgements

The authors gratefully acknowledge the financial support provided by the Natural Science Foundation of China (National Key Project No.11032005).

References

[1] Carpinteri A, Cornetti P, Lacidogna G, Paggi M. Towards a unified approach for the analysis of failure modes in FRP-retrofitted concrete beams. Adv Struct Eng 2009;12:715–29.
[2] Chajes MJ, Finch WW, Januszka TF, Thomson TA. Bond and force transfer of composite material plates bonded to concrete. ACI Struct J 1996;93(2):208–17.
[3] Bizindavyi L, Neale KW. ransfer lengths and bond strengths for composite bonded to concrete. J Compos Constr ASCE 1999;39(4):; 153–160.
[4] Yoshizawa H, Wu ZS, Yuan H. Study on FRP-concrete interface bond performance. J Mater Concr Struct Pavements, JSCE 2000;49(662):105–19.
[5] Nakaba K, Kanakubo T, Furuta T, Yoshizawa H. Bond behavior between fiber-reinforced polymer laminates and concrete. ACI Struct J 2001;98(3):359–67.
[6] Yao J, Teng JG, Chen JF. Experimental study on FRP-to-concrete bonded joints. Compos Part B: Eng 2005;36(2):99–113.
[7] Täljsten B. Strengthening of concrete prisms using the plate-bonding technique. Int J Fract 1996;82:253–66.
[8] Brosens K, Van GD. Plate end shear design for external CFRP laminates. In: Proceedings of FRAMCOS-3. Freiburg, Germany: Aedificatio Publishers; 1998. p. 1793–804.
[9] Yuan H, Wu ZS, Yoshizawa H. Theoretical solutions on interfacial stress transfer of externally bonded steel/composite laminates. J Struct Mech Earthquake Eng JSCE 2000;18(1):27–39.
[10] Wu ZS, Yuan H, Niu H. Stress transfer and fracture propagation in different kinds of adhesive joints. J Eng Mech ASCE 2002;128(5):562–73.
[11] Chirstopher KYL, Tung WK. A three-parameter model for debonding of FRP from concrete substrate. FRP Compos Civil Eng 2001;I and II:373–9.
[12] Teng JG, Chen JF, Smith ST, Lam L. Behaviour and strength of FRP-strengthened RC structures: a state-of-the-art review. Proc Inst Civil Eng-Struct Build 2003;156(1):51–62.
[13] Yuan H, Teng JG, Seracino R, Wu ZS, Yao J. Full-range behavior of FRP-to-concrete bonded joints. Eng Struct 2004;26(5):553–65.
[14] Leung CKY, Tung WK. Three-parameter model for debonding of FRP plate from concrete substrate. J Eng Mech ASCE 2006;132:509–18.
[15] Cornetti P, Carpinteri A. Modelling the FRP-concrete delamination by means of an exponential softening law. Eng Struct 2011;33(6):1988–2001.
[16] Woo SK, Lee Y. Experimental study on interfacial behavior of CFRP-bonded concrete. J Civil Eng, KSCE 2010;14(3):385–93.